Inorg. Chem. **2006**, *45*, 7464–7479

An ab Initio Molecular Dynamics and Density Functional Theory Study of the Formation of Phosphate Chains from Metathiophosphates

Nicholas J. Mosey and Tom K. Woo*

Department of Chemistry, The University of Western Ontario, London, Ontario, Canada N6A 5B7

Received May 15, 2006

The reactions that occur between metathiophosphate (MTP) molecules are identified and examined through ab initio molecular dynamics simulations and static quantum chemical calculations at the density functional level of theory. The simulations show that certain types of MTPs can react to yield phosphate chains, while others only dimerize. These differences are rationalized in terms of reaction energies and the electronic structures of these molecules. In the reaction leading to the formation of phosphate chains, the reactive center, a tri-coordinate phosphorus atom, is continually regenerated. A polymerization mechanism linking MTPs to phosphate chains is developed on the basis of these results. This information sheds light on the underlying processes that may be responsible for the formation of phosphates under high-temperature conditions and may prove useful in the development of protocols for the rational synthesis of complex phosphate structures.

I. Introduction

Phosphates comprise an important class of inorganic materials that are of technological and industrial relevance. These materials adopt a number of geometric configurations including chains, cyclic structures, porous networks, and glasses. Crystalline phosphates are used in areas such as heterogeneous catalysis,[1] molecular separation,[2] and other technologies.[3] Meanwhile, amorphous phosphates are the basis of glasses used in optical applications,[4] incorporated into biological implants,[5] and primary components of engine antiwear films.[6] Many protocols have been developed for the formation of amorphous and crystalline phosphates.[7] These procedures typically involve heating appropriate phosphorus-containing precursors to promote polymerization reactions that yield the various structures mentioned above.

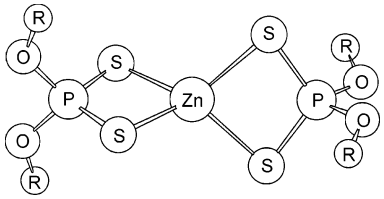

Figure 1. General structure of the ZDDP molecule. The label R denotes an alkyl group.

However, many of the key molecular-level processes involved in the formation of phosphates remain poorly understood due to the large number of variables associated with these processes and the difficulty in studying these systems directly under commonly used reaction conditions.[8] A detailed understanding of the fundamental processes involved in the transformation of basic phosphorus-containing molecules into larger, more complex phosphate species will prove valuable in devising selective synthetic protocols.

Our interest in phosphates stems from the fact that they are the main components of antiwear films formed in automobile engines. These films are derived from motor oil additives called zinc dialkyldithiophosphates (ZDDPs) and have been the focus of intense study for over 70 years.[6,9,10] The ZDDP molecule is shown in Figure 1 and has the chemical formula $Zn[S_2P(OR)_2]_2$, where R indicates an alkyl

* To whom correspondence should be addressed. E-mail: twoo@uottawa.ca. Current address: Department of Chemistry, University of Ottawa, D'Iorio Hall, 10 Marie-Curie, Ottawa, Ontario, Canada K1N 6N5.

(1) Guillou, N.; Gao, Q.; Forster, P. M.; Chang, J. S.; Nogues, M.; Park, S. E.; Ferey, G.; Cheetham, A. K. *Angew. Chem., Int. Ed.* **2001**, *20*, 2831.
(2) Forster, P. M.; Eckert, J.; Chang, J. S.; Park, S. E.; Ferey, G.; Cheetham, A. K. *J. Am. Chem. Soc.* **2003**, *125*, 1309.
(3) Davis, M. E. *Nature* **2002**, *417*, 813.
(4) Campbell, J. H.; Suratwala, T. I.; Thorsness, C. B.; Hayden, J. S.; Thorne, A. J.; Cimino, J. M.; Marker, A. J., III; Takeuchi, K.; Smolley, M.; Ficini-Dorn, G. F. *J. Non-Cryst. Solids* **2000**, *263*−*264*, 342.
(5) Ahmed, I.; Collins, C. A.; Lewis, M. P.; Olsen, I.; Knowles, J. C. *Biomaterials* **2004**, *25*, 3223.
(6) Nicholls, M. A.; Do, T.; Norton, P. R.; Kasrai, M.; Bancroft, G. M. *Tribol. Int.* **2005**, *38*, 15.
(7) Murugavel, R.; Walawalkar, M. G.; Dan, M.; Roesky, H. W.; Rao, C. N. R. *Acc. Chem. Res.* **2004**, *37*, 763.
(8) Norquist, A. J.; O'Hare, D. *J. Am. Chem. Soc.* **2004**, *126*, 6673.
(9) Spikes, H. *Tribol. Lett.* **2004**, *17* (3), 469.
(10) Barnes, A. M.; Bartle, K. D.; Thibon, V. R. A. *Tribol. Int.* **2001**, *34* (6), 389−395.

10.1021/ic0608391 CCC: $33.50
Published on Web 07/25/2006

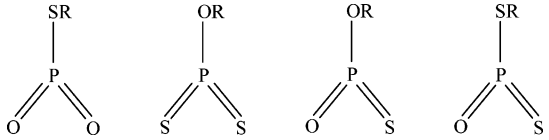

Figure 2. Metathiophosphate molecules that are considered in this study. These molecules can be formed through the decomposition of the ZDDP molecule or its linkage isomers as discussed in a previous study.[17] In all cases, the label R refers to an alkyl group.

substituent. It is generally thought that these additives decompose thermally to yield phosphorus-containing species which then undergo various reactions to yield (zinc) phosphates. The zinc phosphates collect on surfaces where they are transformed under engine conditions into zinc phosphate films. The films exhibit beneficial properties with respect to wear inhibition, such as forming preferentially at locations on engine surfaces where they are needed most and becoming harder to protect surfaces when conditions arise that are most likely to induce wear. As such, these films have been described as 'smart' materials.[11]

Recently, environmental considerations and technological advances have necessitated the replacement of ZDDPs in engine oils.[12−16] The rational development of new antiwear additives requires an understanding of how ZDDP films form and work. We have performed a series of chemical simulation studies[17−21] in an effort to gain useful molecular-level insight into the formation and functionality of these films. The simulations have shed light on molecular-level processes involved in the decomposition of ZDDP, the reactions that transform certain decomposition products into zinc phosphates, and pressure-induced processes that account for both the transformation of the zinc phosphates into films and subsequent wear inhibition. The results of these theoretical studies complement experimental results,[22] and it is our hope that these data can be used in tandem to develop a complete understanding of ZDDP additives and films.

In a recent study,[17] we demonstrated that ZDDP molecules, and isomers thereof, can decompose at high temperatures through the elimination of metathiophosphates (MTPs), such as those shown in Figure 2. MTPs contain a low-coordinate, electrophilic phosphorus atom, as well as oxygen or sulfur atoms that can behave as nucleophiles. It is possible that these components of MTPs will react to yield P−O−P or P−S−P linkages, which are necessary for the formation of phosphates.[23] In this study, we will perform a series of calculations to explore the possible transformation of MTP molecules into more complex phosphate structures.

The calculations will proceed in a manner which is similar to that used in our earlier studies. That is, the chemical behavior of systems composed of the molecules shown in Figure 2 will first be explored through ab initio molecular dynamics (AIMD) simulations.[24,25] This method is a powerful tool for the identification of unknown chemical reactions. Once the relevant reactions are identified through the AIMD simulations, additional static quantum chemical calculations will be performed using density functional theory (DFT). These calculations will provide greater quantitative insight into the energetics associated with these reactions.

The results of the calculations shed light on new and interesting reaction pathways which transform the molecules shown in Figure 2 into phosphate structures. In particular, it will be shown that systems composed entirely of $RSPO_2$ can take part in a polymerization reaction that yields phosphate chains. Interestingly, the other alkyl MTPs do not react similarly. The origins of these differences are explained on the basis of the electronic structures of these molecules. The reactions identified in the calculations will also be used in conjunction with those reported in previous studies to develop a reaction mechanism linking the ZDDP molecule to phosphate precursors to the antiwear films. However, the mechanisms described in this study involve MTP molecules and thus are not unique to the formation of ZDDP antiwear films. As such, these reactions may also prove useful in understanding or controlling the formation of phosphate chains that can act as the basis for amorphous and crystalline phosphate used in applications such as those described above.

The remainder of this paper is as follows. The computational details are given in Section II. The results of the calculations are presented and discussed in Section III. In that section, the basic reactions in which two MTP molecules can take part will be considered first, followed by an examination of the reactions that can take place between the products of these bimolecular reactions and additional MTP molecules to yield longer phosphate chains. A general mechanism for the formation of phosphate chains from MTPs is then developed. The conclusions are presented in Section IV.

II. Computational Details

AIMD simulations were performed within the Car−Parrinello extended Lagrangian formalism[26] using the CPMD software package, version 3.5.[27] The potential energy was calculated using Kohn−Sham DFT[28,29] with the gradient-corrected exchange-correlation functional of Perdew, Burke, and Ernzerhof, which is commonly abbreviated as PBE.[30] The core electrons of all atoms were replaced

(11) Bec, S.; Tonck, A.; Georges, J. M.; Coy, R. C.; Bell, J. C.; Roper, G. W. *Proc. R. Soc. London, Ser. A* **1999**, *455*, 4181.
(12) Nicholls, M. A.; Norton, P. R.; Bancroft, G. M.; Kasrai, M. *Wear* **2004**, *257*, 311.
(13) Wan, Y.; Cao, L.; Xue, Q. *Tribol. Int.* **1998**, *30* (10), 767−772.
(14) Fuller, M.; Kasrai, M.; Sheasby, J. S.; Bancroft, G. M.; Fyfe, K.; Tan, K. H. *Tribol. Lett.* **1995**, *1*, 367.
(15) Schey, J. A.; Nautiyal, P. C. *Wear* **1991**, *146* (1), 37−51.
(16) Inoue, K.; Kurahashi, T.; Negishi, T.; Akiyama, K.; Arimura, K.; Tasaka, K. *SAE* **1992**, 920654.
(17) Mosey, N. J.; Woo, T. K. *Tribol. Int.*, in press.
(18) Mosey, N. J.; Müser, M. H.; Woo, T. K. *Science* **2005**, *307*, 1612.
(19) Mosey, N. J.; Woo, T. K. *Inorg. Chem.* **2005**, *44*, 7274.
(20) Mosey, N. J.; Woo, T. K. *J. Phys. Chem. A* **2004**, *108*, 6001−6016.
(21) Mosey, N. J.; Woo, T. K. *J. Phys. Chem. A* **2003**, *107* (25), 5058−5070.
(22) Mosey, N. J.; Woo, T. K.; Kasrai, M.; Norton, P. R.; Müser, M. H. *Tribol. Lett.*, in press.
(23) In this study, the term phosphate will be used in a general sense to represent both phosphates, which contain P−O−P linkages, and thiophosphates, which contain P−S−P linkages.
(24) Tse, J. S. *Annu. Rev. Phys. Chem.* **2002**, *53*, 249−290.
(25) Tuckerman, M. E. *J. Phys.: Cond. Mater.* **2002**, *14* (50), R1297−R1355.
(26) Car, R.; Parrinello, M. *Phys. Rev. Lett.* **1985**, *55* (22), 2471−4.
(27) Hütter, J.; Alavi, A.; Deutsch, T.; Bernasconi, M.; Gödecker, S.; Marx, D.; Tuckerman, M.; Parrinello, M. *CPMD version 3.5*; MPI für Festkörperforschung and IBM Zurich Research Laboratory: Zurich, 1995−2001.

by analytic pseudopotentials,[31,32] while the valence space was represented by a set of plane waves expanded up to a kinetic energy cutoff of 70 Ry. Previously, we have found that this computational methodology yields accurate energetics for the dimerization, isomerization, and decomposition of ZDDPs.[17,21,33] All simulations were performed using a face-centered cubic cell, and a super-cell approach was employed to avoid spurious interactions between periodic neighbors. In all cases, the cell size for the AIMD simulations was selected such that the shortest distance between atoms in neighboring cells was at least 7 Å at the start of a simulation. Geometric constraints were applied using the RATTLE algorithm[34] as implemented in CPMD, and the use of these constraints will be described as appropriate in what follows. A time step of 6.0 au, equivalent to 0.145 fs, was used in all AIMD simulations, which maintained energy conservation to within $\pm 1 \times 10-5$ au/ps or better. To give the reader an idea of the computational effort associated with these simulations, it is noted that nearly 7000 energy and force evaluations are required to perform 1 ps of simulation with a time step of the size used here. In terms of real time, 1 ps of simulation required approximately 48 h of calculation on a 16 CPU cluster of Compaq Alpha ES40 computers running at 833 MHz.

All AIMD simulations were performed in the NVE ensemble with the kinetic energy of the system equivalent to a temperature of approximately 500 K at the start of the production portion of the simulation. This is similar to average surface temperatures in engines[35] and hence is suitable for these simulations. To equilibrate the systems, the initial nuclear velocities were randomly selected from a Maxwell−Boltzmann distribution at 100 K and a 0.5 ps simulation was performed where the temperature was held at 100 ± 50 K through rescaling of the nuclear velocities. Once this portion of the equilibration was completed, the velocities were rescaled instantaneously to correspond to a temperature of 300 K and a further 0.5 ps of simulation was performed, where once again, the temperature was maintained within 50 K through velocity rescaling. For the final part of the equilibration, the nuclear velocities were once again rescaled instantaneously to give a temperature of 500 K and a 1.0 ps simulation was performed with the temperature held within 50 K of 500 K. Once this portion of the simulation was completed, the system was allowed to evolve without any constraints on the temperature until a chemical reaction was observed. All of the results of the AIMD simulations that are reported in this study were obtained from this final portion of the simulation.

Static DFT calculations were performed with the Jaguar 5.0 software package.[36] The exchange−correlation functional commonly abbreviated as B3LYP, which is composed of Becke's three-parameter hybrid gradient-corrected exchange functional[37] and the gradient-corrected correlation functional of Lee, Yang, and Parr, was used for these calculations.[38] A 6-311+G(d,p) basis set was used on all atoms.

The products of the observed reactions may adopt a large number of different conformations. To account for this, a systematic scheme was used in an effort to locate a global minimum when optimizing the structures of the products. Within this geometry optimization scheme, a 1.0 ns molecular dynamics simulation was performed at 1000 K using the Universal 1.02 force field[39] in the Cerius2 molecular modeling package.[40] One hundred structures were selected at regular intervals along the resulting trajectory and optimized at the PM3 semiempirical level of theory[41,42] with the Gaussian 98 suite of programs.[43] The 10 unique lowest energy structures were then optimized with DFT methods as described above. The data corresponding to the lowest energy DFT structure is reported in what follows. This procedure does not guarantee the location of a global minimum; however, it does allow for the consideration of a large number of structures in an automated fashion, which should decrease the errors that would likely be introduced by assuming that one particular conformation is the most stable. The global optimization scheme was not used in the determination of the structures of the intermediates and transition states, which were based on the geometries of the products.

Frequency calculations were performed to characterize all stationary points and to estimate zero-point vibrational energy (ZPVE) corrections, which are included unscaled in all reported energies. The free energies at temperatures of 500 and 1000 K and a pressure of 1 atm were calculated within the ideal gas approximation during the frequency calculations to estimate the effect of temperature on the energetics of the observed reactions. Such effects are relevant to the current study since the ZDDP molecules react at high temperatures under typical engine conditions. The temperature of 500 K is similar to average engine temperatures[35] and is also comparable to those used to generate thermal films in laboratory experiments, while the temperature of 1000 K is an estimate of those encountered at points of microscopic contact within the engine.

ZDDPs can be produced with a variety of different substituents, which will be found in the MTP molecules derived through the

(28) Kohn, W.; Sham, L. J. *Phys. Rev.* **1965**, *140*, A1133-A1138.
(29) Hohenberg, P.; Kohn, W. *Phys. Rev.* **1964**, *136*, B864−B871.
(30) Perdew, J. P.; Burke, K.; Ernzerhof, M. *Phys. Rev. Lett.* **1996**, *77* (18), 3865−3868.
(31) Hartwigsen, C.; Gödecker, S.; Hütter, J. *Phys. Rev. B* **1998**, *58* (7), 3641−3662.
(32) Gödecker, S.; Teter, M.; Hütter, J. *Phys. Rev. B* **1996**, *54* (3), 1703−1710.
(33) Previously, we have used this methodology in a study of the relative, stabilities of ZDDP monomers and dimers,[21] and it was found that the dimerization energies calculated at the PBE/70 Ry level of theory agreed within 2.0 kcal/mol of those calculated using all-electron representations of the wave function at the PBE/TZP level of theory. We have also tested this methodology by evaluating the energetics associated with various isomerization and decomposition reactions involving the ZDDP molecule.[17] Specifically, we have studied the isomerization of the hydrogen-substituted ZDDP molecule and the decomposition of methyl-substituted ZDDP to yield DDP−Zn−OMe + $MeOPS_2$. In the case of the isomerization reaction, energies of 6.0, 4.4, and 3.4 kcal/mol were calculated at the PBE/70 Ry, PBE/200 Ry, and PBE/LACV3P+(d,p) levels, respectively. For the decomposition of methyl-substituted ZDDP, which involves significant changes in the bonding arrangements and hybridizations at key atoms in the system, reaction energies of 53.7, 56.6, and 54.8 kcal/mol were evaluated at the PBE/70 Ry, PBE/200 Ry, and PBE/LACV3P+(d,p) levels, respectively. The agreement between these values is suitable within the qualitative context of our simulations.
(34) Andersen, H. C. *J. Comput. Phys.* **1983**, *52* (1), 24−34.
(35) McGeehan, J. A.; Graham, J. P.; Yamaguchi, E. S. *SAE* **1990**, 2310.
(36) *Jaguar 5.0*; Schrodinger, LLC: Portland, OR, 2002.
(37) Becke, A. D. *J. Chem. Phys.* **1993**, *98* (7), 5648−52.
(38) Lee, C.; Yang, W.; Parr, R. G. *Phys. Rev. B* **1988**, *37* (2), 785−9.
(39) Castonguay, L. A.; Rappe, A. K. *J. Am. Chem. Soc.* **1992**, *114*, 5832.
(40) *Cerius2_4.2 Modeling Environment*; Molecular Simulations, Inc.: San Diego, 1999.
(41) Stewart, J. J. P. *J. Comput. Chem.* **1989**, *10*, 209.
(42) Stewart, J. J. P. *J. Comput. Chem.* **1989**, *10*, 221.
(43) Frisch, M. J.; Trucks, G. W.; Schlegel, H. B.; Scuseria, G. E.; Robb, M. A.; Cheeseman, J. R.; Zakrzewski, V. G.; Montgomery, J. A., Jr.; Stratmann, R. E.; Burant, J. C.; Dapprich, S.; Millam, J. M.; Daniels, A. D.; Kudin, K. N.; Strain, M. C.; Farkas, O.; Tomasi, J.; Barone, V.; Cossi, M.; Cammi, R.; Mennucci, B.; Pomelli, C.; Adamo, C.; Clifford, S.; Ochterski, J.; Petersson, G. A.; Ayala, P. Y.; Cui, Q.; Morokuma, K.; Malick, D. K.; Rabuck, A. D.; Raghavachari, K.; Foresman, J. B.; Cioslowski, J.; Ortiz, J. V.; Stefanov, B. B.; Liu, G.; Liashenko, A.; Piskorz, P.; Komaromi, I.; Gomperts, R.; Martin, R. L.; Fox, D. J.; Keith, T.; Al-Laham, M. A.; Peng, C. Y.; Nanayakkara, A.; Gonzalez, C.; Challacombe, M.; Gill, P. M. W.; Johnson, B. G.; Chen, W.; Wong, M. W.; Andres, J. L.; Head-Gordon, M.; Replogle, E. S.; Pople, J. A. *Gaussian 98*, revision A.9; Gaussian, Inc.: Pittsburgh, PA, 1998.

decomposition of the ZDDP additive. Typical substituents are primary or secondary alkyl groups of up to approximately 10 carbon atoms in length. In the current study, it is of primary interest to examine the chemical behavior related to the phosphorus, sulfur, and oxygen atoms of the MTP molecules that may lead to the formation of phosphate chains. It is unlikely that the nature of the alkyl group will exert a direct influence on this behavior, at least when typical alkyl substituents are considered, and methyl substituents will be used exclusively in this study to minimize the computational effort associated with these calculations.

III. Results and Discussion

The goal of this study is to identify reactions that transform MTP molecules into more complex phosphates. As noted above, the calculations will focus on the species shown in Figure 2. In Section a, the reactions that occur within bimolecular systems composed of two identical alkyl MTP molecules will be identified and explored using AIMD simulations and static quantum chemical calculations. The results demonstrate that $MeSPO_2$ can participate in bimolecular reactions that form diphosphate chains, while the other three alkyl MTP molecules simply dimerize. In Section b, simulations are reported that were performed to explore the interaction between the products of the bimolecular reactions and additional alkyl MTP molecules. The results demonstrate that species derived from $MeSPO_2$ can take part in reactions leading to the formation of linear phosphate chains. In Section c, the reactions identified through the calculations are considered along with the results reported in previous studies to establish a reaction mechanism which connects the ZDDP molecule to phosphate chains, which is motivated by our particular interests and may be of technological relevance.

a. Bimolecular Reactions of Alkyl MTPs. The natural starting point for a study of the formation of phosphates from alkyl MTPs is to consider the reactions that occur between two identical alkyl MTP molecules. AIMD simulations were performed to identify and examine the qualitative details of such reactions, which to this point have remained largely unknown. One simulation was performed for each type of alkyl MTP shown in Figure 2. To promote the occurrence of chemical reactions within the limited time scales of these simulations (tens of picoseconds), geometric constraints were applied such that the distance between the phosphorus atoms of the two reacting alkyl MTP molecules was only allowed to decrease from an initial value of 7 Å throughout the course of the simulation. Within this scheme, the two phosphorus atoms were not forced to approach one another, but rather the P−P distance decreased only if the nuclear forces allowed this to occur naturally. The constraints were applied to this distance simply on the basis of the notion that the phosphorus atoms must approach one another for a reaction to occur between the two alkyl MTP molecules. It is noted that constraints could have been applied to other geometric variables, such as a P−O or P−S distance; however, it is probable that such a situation would artificially favor the formation of either P−O−P or P−S−P linkages.

The results of the AIMD simulations are presented in Section a.i. and show that the formation of diphosphates from alkyl MTPs can occur through either dimerization or a reaction involving the transfer of a sulfide or alkoxy group between the two phosphorus atoms. Static DFT calculations were performed to examine the energetic and mechanistic details of these reactions, and the results are presented in Section a.ii. Overall, the results of the AIMD simulations and static DFT calculations indicate that the $MeSPO_2$ system may follow either of the two identified reaction pathways, while the other three alkyl MTP molecules in Figure 2 are primarily expected to dimerize. The underlying aspects of the electronic structures of these systems that are responsible for this behavior are examined in Section a.iii.

a.i. AIMD Simulations of Systems Composed of Two Identical Alkyl MTPs. The simulation of the system composed of two $MeSPO_2$ molecules indicated that these two molecules can react to yield a diphosphate chain through the formation of a P−O−P linkage. Key structures along the calculated trajectory that demonstrate this process are shown in Figure 3. In Figure 3a, the system is in a state where the two MTP molecules are separated by a large distance as a result of the initial geometric constraints. As the distance between the two MTP molecules decreased, adducts were observed, such as that in Figure 3b. These species contain a P−O−P linkage yet did not persist for long periods of time. Eventually, the transfer of a sulfide group between the two phosphorus atoms occurred along with the formation of a P−O−P linkage, as shown in Figure 3c. Once this reaction was complete, the geometric constraints were removed and the simulation was continued for 2 ps to determine if the product was a stable species or an artifact of these constraints. The results of this unconstrained simulation showed that the product persisted in the absence of the constraints and adopted the structure shown in Figure 3d. The product is particularly interesting within the context of phosphate chain formation because it contains a tri-coordinate phosphorus atom in an environment which is similar to that in the original $MeSPO_2$ molecule. This is a potential site for the elongation of the phosphate chain through analogous reactions with additional alkyl MTP molecules. These types of reactions are considered in Section b.

Analogous AIMD simulations were performed on systems composed of two $MeOPS_2$, MeOP(S)O, or MeSP(S)O molecules. These three types of alkyl MTPs were all observed to dimerize, as opposed to taking part in the phosphate chain formation reaction observed for $MeSPO_2$. The qualitative details of the dimerization reactions were similar for each of the $MeOPS_2$, MeOP(S)O, and MeSP(S)O bimolecular systems, and for the sake of brevity, only the data for $MeOPS_2$ will be considered explicitly.

Key structures observed during the simulation of the system composed of two $MeSPO_2$ molecules are shown in Figure 4. The structure in Figure 4a shows that the two MTP molecules were well-separated, which was due to the initial geometric constraints. As the intermolecular distance decreased, the system adopted structures such as that in Figure 4b, which were consistent with the transfer of a methoxy group and formation of a P−S−P linkage through a process analogous to that described above for $MeSPO_2$. Despite the formation of such structures, chain formation did not occur,

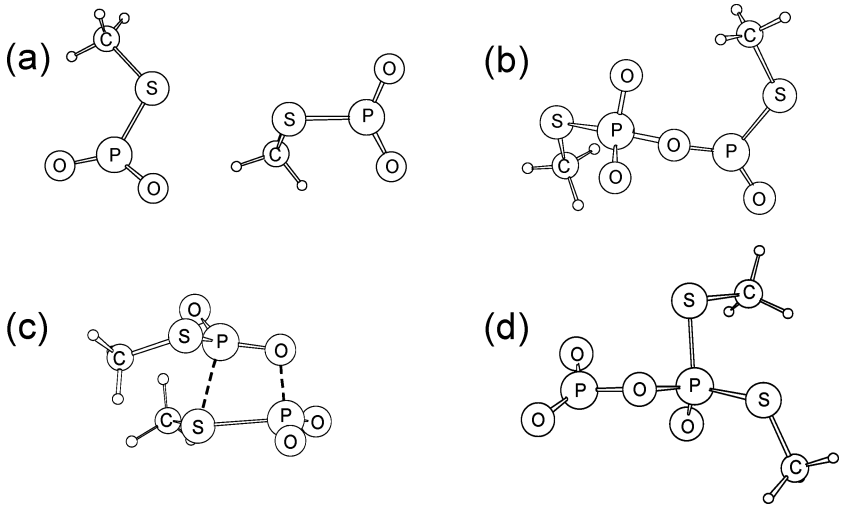

Figure 3. Key structures observed during the AIMD simulation of the $MeSPO_2$ system. In (a) through (c), the P−P distance is subject to geometric constraints. In (a), the two MTP molecules are separated by a significant distance as a result of the initial geometric constraints. Throughout the simulation, structures that contained a P−O−P linkage were observed, such as that in (b); however, these did not persist or lead to the formation of phosphates. In (c), the system attained a configuration that allowed for the transfer of a sulfide group and simultaneous formation of a P−O−P linkage. The product of this reaction is shown in (d) and was obtained after the removal of the geometric constraints.

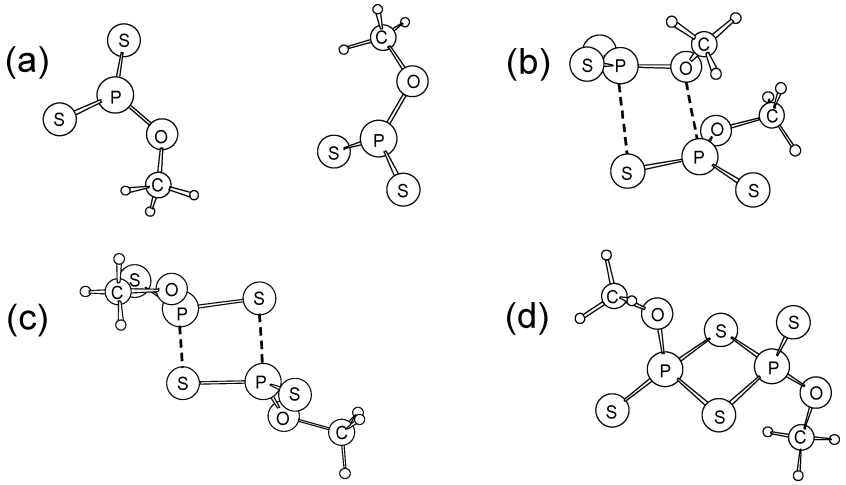

Figure 4. Key structures observed during the simulation of the $MeOPS_2$ system. In (a) through (c), the P−P distance is subject to geometric constraints. In (a), the two molecules are separated by a significant distance. At an early stage of the simulation, a structure consistent with methoxy group transfer and P−S−P linkage formation were observed, as in (b); however, this process did not occur. In (c), the system has attained a configuration allowing for dimerization through the formation of two P−S bonds. The final product, obtained after the removal of the geometric constraints, shown in (d), contains a P−S−P−S four-membered ring and is referred to as a dithiadiphosphetane.

which is indicative of a significant energy barrier to that process for the $MeOPS_2$ system. Eventually, the system adopted an alternate configuration that led to the nearly simultaneous formation of two P−S bonds, as shown in Figure 4c. The final product, which was obtained by removing the geometric constraints and continuing the simulation for 2 ps after the formation of the P−S bonds took place, is shown in Figure 4d. The product is simply the dimeric structure of $MeOPS_2$, called a dithiadiphosphetane. Analogous structures containing P−O−P−S four-membered rings, referred to as thiaoxadiphosphetanes, were formed during the simulations of the MeOP(S)O and MeSP(S)O systems. Structures containing these types of four-membered rings have been reported previously;[44−46] however, to the best of our knowledge, the relevance of these species within the context of phosphate formation has not been examined.

a.ii. Static DFT Calculations of the Reactions Between Two Identical MTPs. The results of the AIMD simulations shed light on two different reaction pathways leading to the formation of diphosphates from systems composed of two identical alkyl MTP molecules. In the first reaction, a sulfide or alkoxy group is transferred between the two phosphorus atoms, which prompts the formation of a P−O−P or P−S−P linkage. In the second reaction, the two MTP molecules simply dimerize. These reactions are outlined in Scheme 1 as reactions **1** and **2**, respectively, and will be referred to as chain formation and dimerization. Due to the limited nature of the AIMD simulations, i.e., only one short simulation per type of MTP, it is not possible to conclude that the observed reactions are absolutely representative of the typical behavior

(44) Nizamov, I. S.; Sergeenko, G. G.; Popovich, A. E.; Nizamov, I. D.; Batyeva, E. S.; Al′fonsov, V. A. *Russ. J. Gen. Chem.* **2002**, *72* (9), 1356−1366.
(45) Beckmann, H.; Ohms, G.; Grossmann, G.; Krueger, K.; Klostermann, K.; Kaiser, V. *Heteroatom Chem.* **1996**, *7* (2), 111−18.
(46) Powell, J.; Ng, K. S.; Sawyer, J. F. *J. Chem. Soc. Chem. Commun.* **1987** (14), 1131−2.

Scheme 1. Reactions Identified during the AIMD Simulations of the Alkyl MTPs[a]

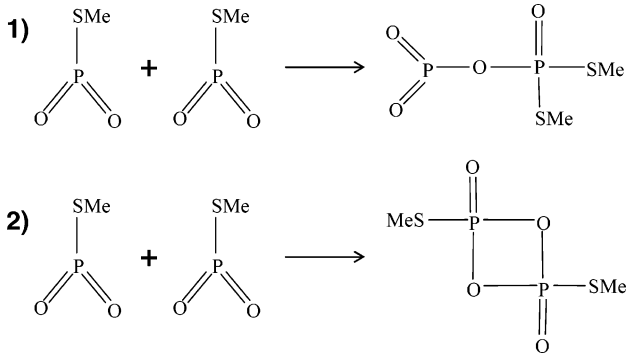

[a] These reactions are outlined explicitly for the $MeSPO_2$ system; however, analogous processes are possible for the other alkyl MTPs. Reaction **1** yields a phosphate chain through the formation of a P−O−P linkage, which is prompted by the transfer of the sulfide group. Reaction **2** involves the dimerization of the MTP molecules.

of these species. Unfortunately, it is not computationally feasible to obtain statistically meaningful data by performing a large number of AIMD simulations. However, it is possible to gain such insight through an analysis of the energetic details associated with the observed reactions. To achieve this, the stationary points along the mechanistic pathways associated with reactions **1** and **2** were calculated at the B3LYP/6-311+G(d,p) level of theory. The structural details of these species, given in Figures 5 and 6, will be considered first in order to gain a general understanding of these reactions. An examination of the energetics of these reactions, given in Tables 1 and 2, then follows.

The stationary points along the mechanistic pathways for reaction **1** are shown in Figure 5 for each of the alkyl MTP molecules considered in this study. In all cases, the products of these reactions have structures that are consistent with those expected on the basis of the results of the AIMD simulation of $MeSPO_2$, where this reaction was actually observed. The geometric details of the transition states are qualitatively similar regardless of the nature of the parent MTP molecule, and in general, the formation of the P−O−P or P−S−P linkage occurs at approximately the same time as the transfer of the sulfide or methoxy group. When this is considered in conjunction with the fact that only one transition state structure was located for each reaction, it is possible to conclude that chain formation occurs in a concerted fashion. It was found that the degree of bond formation in the adduct exhibited a dependence upon the nature of the MTP molecule, with these species adopting geometries in which the P−O bonds were formed to a significantly greater extent than the P−S bonds, at least upon comparison to the respective bond distances in the products. This is most likely due to differences in the long-range P−O and P−S electrostatic interactions, which dominate in these weakly bound structures, with the P−O interaction being stronger than the P−S interaction.

The structures located along the mechanistic pathways for reaction **2** are shown in Figure 6 for each of the alkyl MTP molecules. In all cases, the products have structures that are consistent with those expected on the basis of the AIMD simulations of the $MeOPS_2$, MeOP(S)O, and MeSP(S)O systems, where dimerization actually occurred. The transition states characterize the nature of this reaction, and in all cases, the geometric details associated with these structures indicate that bond formation occurs in a concerted fashion. In the transition-state structures given in Figure 6a and b, the four atoms involved in the formation of the four-membered ring have adopted a nearly planar configuration, which is consistent with that in the product. Meanwhile, the geometric details of the transition state structures shown in Figure 6c and d indicate that the two MTP molecules must rotate relative to one another along the reaction pathway between this species and the product. The adducts shown in Figure 6a and b have structures consistent with the early stages of concerted bond formation, while in the adduct structures shown in Figure 6c, the P−O bond is formed to a more substantial degree than the P−S bond, based on the interatomic distances. As suggested above, this is most likely due to differences in the P−O and P−S electrostatic interactions. During the dimerization of MeOP(S)O and MeSP(S)O to yield dithiadiphosphetanes, as shown in Figure 6d, it was found that the system proceeds directly through the transition state without forming an adduct.

The calculated electronic potential energies and free energies of the stationary points located along the mechanistic pathways for reactions **1** and **2** are given in Tables 1 and 2, respectively, relative to the separate MTP molecules. One of the most obvious features of the energetics is that all of the reactions are disfavored thermodynamically and kinetically at 1000 K. This is not particularly surprising, given that the entropic contribution to the free energy is significant at such high temperatures and disfavors association reactions. However, this observation is important because it was found previously that alkyl MTP molecules are only likely to be formed at temperatures approaching 1000 K.[17] This suggests that, once formed, the MTP molecules should not dimerize or form chains immediately, but instead they should persist in the oil until they encounter lower-temperature regions where these reactions can take place. This may allow for appreciable quantities of MTP molecules to accumulate within the engine, which creates an ideal environment for the formation of phosphates through the reactions considered here, assuming that other reactions will not take place at elevated temperatures to remove the MTP molecules from the system. This is a reasonable assumption because the unfavorable energetics at 1000 K are due primarily to entropic contributions to the free energy and similar entropic penalties will be incurred during other bimolecular reactions. Since the energetics at 1000 K indicate that both reactions are disfavored for all species, the following analysis will focus exclusively on the ΔE and ΔG^{500K} values.

The ΔE data for the $MeSPO_2$ system show that the chain formation and dimerization reactions are both highly favored on the electronic potential energy surface. The overall kinetics and thermodynamics favor dimerization (reaction **2**); however, the relative electronic potential energies of the adducts formed along each pathway favor progression towards the formation of phosphate chains (reaction **1**). Since all points along both reaction pathways lie lower in electronic

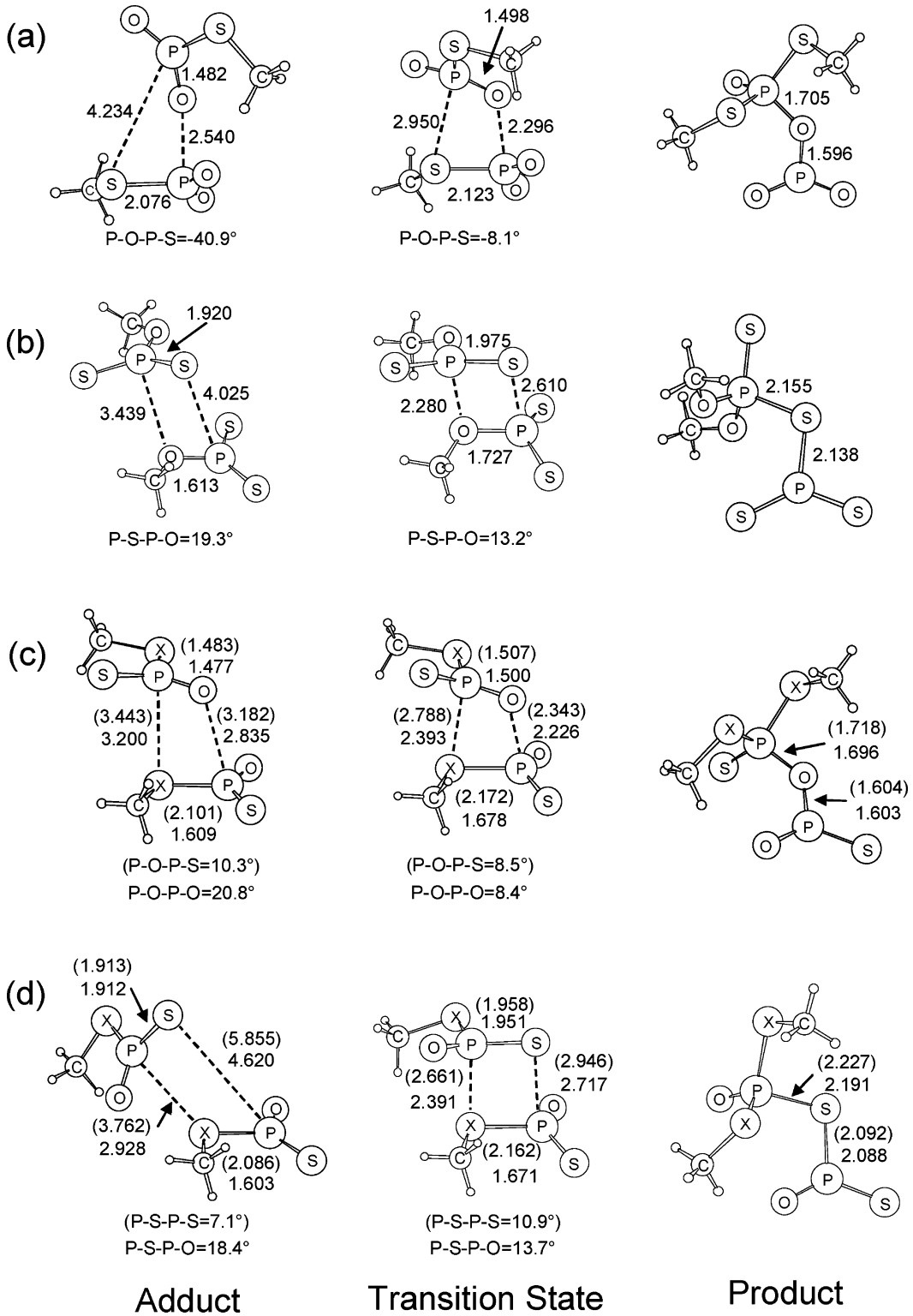

Figure 5. Structures of the stationary points along the mechanistic pathways for reaction **1**. In (a), the structures for $MeSPO_2$ system are shown. In (b), the structures for the analogous reaction involving $MeOPS_2$ molecules are given. In (c), the structures for the reaction of either MeOP(S)O (X = O) or MeSP(S)O (X = S) molecules to yield products with P−O−P linkages are shown. In (d), the structures for the reaction of either MeOP(S)O (X = O) or MeSP(S)O (X = S) molecules to yield products with P−S−P linkages are given. In (c) and (d), the values for the MeSP(S)O system are provided in parentheses. All distances are in Å, and the first atom in the dihedral values below each structure corresponds to that in the top left corner of the four atoms that form the dihedral angle with the other atoms in the label following in a clockwise direction.

potential energy than the reactants, it is difficult to determine which reaction is favored using these data. Within the context of our interest in ZDDP antiwear additives, the free energies at 500 K are more relevant because this is similar to average engine surface temperatures under operating conditions.[35] The relative free energies at 500 K clearly favor dimerization in terms of overall thermodynamics, and hence, it is anticipated that the system will preferentially adopt the dimeric structure when the system is at equilibrium. This may appear to contrast with the results of the AIMD simulations, where

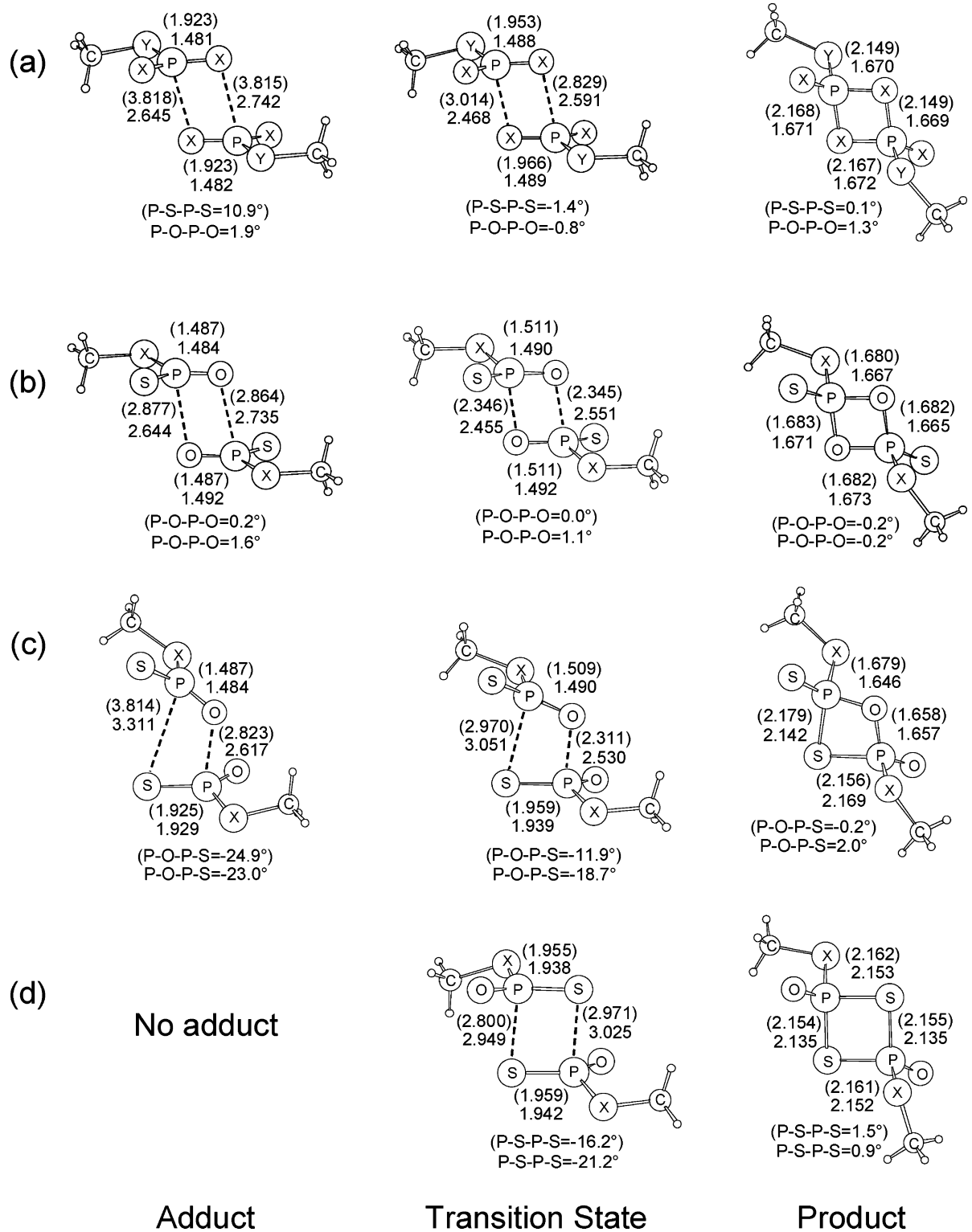

Figure 6. Structures of the calculated stationary points along the mechanistic pathways for reaction **2**. In (a), the structures for the dimerization of $MeSPO_2$ (X = O and Y = S) and $MeOPS_2$ (X = S and Y = O) are shown. In (b), the structures for the dimerization of MeOP(S)O (X = O) and MeSP(S)O (X = S) to yield products with P−O−P−O four-membered rings are shown. In (c), the structure for the dimerization of MeOP(S)O (X = O) and MeSP(S)O (X = S) to yield products with P−S−P−O four-membered rings are shown. In (d), the structures for the dimerization of MeOP(S)O (X = O) and MeSP(S)O (X = S) to yield products with P−S−P−S four-membered rings are shown. All distances are in Å, and the first atom in the given dihedral value corresponds to that in the top left corner of the four atoms that form the dihedral angle with the other atoms in the label following in a clockwise direction.

chain formation was observed. However, the barriers to reactions **1** and **2** are similar (20.8 and 18.3 kcal/mol, respectively, with respect to the energies of the separate $MeSPO_2$ molecules), which indicates that the reactions should proceed at somewhat competitive rates, given the accuracy of the computational methodology. Thus, reactions **1** and **2** are competitive kinetically for the $MeSPO_2$ system, and one would anticipate observing the formation of both dimers and diphosphate chains on short time scales, while the overall reaction energies indicate that the products of reaction **1** are

Table 1. Relative Electronic and Free Energies[a,b] for the Formation of Phosphate Chains from Alkyl MTPs through Reaction **1**

species	ΔE	ΔG^{500K}	ΔG^{1000K}
$2MeSPO_2 \rightarrow O_2P-O-P(O)(SMe)_2$			
adduct	−6.7	17.2	41.8
transition state	−3.5	20.8	45.8
product	−15.5	10.0	36.6
$2MeOPS_2 \rightarrow S_2P-S-P(S)(OMe)_2$			
adduct	−1.4	21.7	44.3
transition state	8.5	34.5	61.4
product	−13.7	9.4	31.2
$2MeOPS_2 \rightarrow S(O)P-O-P(S)(OMe)_2$			
adduct	−3.0	22.0	49.0
transition state	0.8	25.5	51.2
product	−24.1	−0.1	24.3
$2MeOP(S)O \rightarrow S(O)P-S-P(O)(OMe)_2$			
adduct	−3.7	19.7	43.9
transition state	2.9	27.7	53.4
product	−19.5	4.1	27.7
$2MeSP(S)O \rightarrow S(O)P-O-P(S)(SMe)_2$			
adduct	−0.3	23.1	46.2
transition state	3.7	26.3	47.3
product	−12.3	11.1	33.4
$2MeSP(S)O \rightarrow S(O)P-S-P(O)(SMe)_2$			
adduct	1.5	30.0	63.8
transition state	7.2	31.0	54.4
product	−6.2	18.1	42.3

[a] All energies are in kcal/mol relative to separate reactant molecules at the B3LYP/6-311+G(d,p) level of theory and include ZPVE corrections. [b] The superscripted numbers on the free energy headings in the table indicate the temperature at which the free energy was calculated.

not likely to exist in large quantities when the system reaches chemical equilibrium on longer time scales. As such, the products of reaction **1** should be considered as kinetically accessible transient species formed during the reaction between two $MeSPO_2$ molecules, which is consistent with the results of additional simulations and analysis discussed below.

The data for the $MeOPS_2$ system indicate that dimerization (reaction **2**) is favored both kinetically and thermodynamically on the electronic potential energy surface. Once again, the adduct for chain formation (reaction **1**) is favored over that along the dimerization reaction pathway (reaction **2**), which can be understood in terms of atomic charges. In this case, however, the barrier separating the adduct from the product of chain formation ($\Delta E^{\ddagger} = 9.9$ kcal/mol) will slow the reaction significantly and may allow for dimerization to occur instead. In fact, this is what was observed during the AIMD simulations (see structures b and c in Figure 4). The free energies at 500 K, which are more relevant when discussing the behavior under engine conditions, indicate that the separated reactant molecules are more stable than either of the dimerization or chain formation products. As a result, it is unlikely that either of these products will exist after sufficiently long periods of time.

The MeOP(S)O and MeSP(S)O systems can each undergo chain formation to yield either of two products or they can dimerize to yield any of three dimers. For MeOP(S)O, the electronic potential energies and the free energies at 500 K clearly favor dimerization to yield either dioxadiphosphetane or thiaoxadiphosphetane (P−O−P−O or P−S−P−O rings, respectively). Overall, the kinetics favor the dioxadiphosphetane product, while the thiaoxadiphosphetane product is

Table 2. Relative Electronic and Free Energies[a,b] for the Formation of Phosphates through the Dimerization of Alkyl MTPs through Reaction **2**

species	ΔE	ΔG^{500K}	ΔG^{1000K}
$2MeSPO_2 \rightarrow MeS(O)PO_2P(O)SMe$			
adduct	−6.0	18.9	45.6
transition state	−5.5	18.3	42.7
product	−29.9	−4.3	21.9
$2MeOPS_2 \rightarrow MeO(S)PS_2P(S)OMe$			
adduct	−1.0	23.3	48.2
transition state	4.7	29.6	55.3
product	−15.2	9.0	32.2
$2MeOP(S)O \rightarrow MeO(O)PS_2P(O)OMe$			
transition state	1.0	25.9	52.6
product	−23.7	1.2	26.2
$2MeOP(S)O \rightarrow MeO(O)PS(O)P(S)OMe$			
adduct	−4.7	21.7	51.3
transition state	−4.1	22.4	52.3
product	−30.3	−3.8	24.4
$2MeOP(S)O \rightarrow MeO(S)PO_2P(S)OMe$			
adduct	−6.6	19.8	49.6
transition state	−6.4	19.1	46.7
product	−30.3	−3.6	25.2
$2MeSP(S)O \rightarrow MeS(O)PS_2P(O)SMe$			
transition state	6.7	31.3	56.6
product	−14.5	9.7	32.7
$2MeSP(S)O \rightarrow MeS(O)PS(O)P(S)SMe$			
adduct	−2.4	20.7	43.3
transition state	0.9	25.9	51.7
product	−20.0	4.5	28.2
$2MeSP(S)O \rightarrow MeS(S)PO_2P(S)SMe$			
adduct	−3.5	20.1	43.4
transition state	−1.1	23.0	46.9
product	−19.6	5.4	29.9

[a] All energies are in kcal/mol relative to separate reactant molecules at the B3LYP/6-311+G(d,p) level of theory and include ZPVE corrections. [b] The superscripted numbers on the free energy headings indicate the temperature at which the free energy was calculated.

favored thermodynamically. The differences are slight, however, and the important point to be taken from these values is that these two dimerization products are likely to be formed through the reaction of two MeOP(S)O molecules, while chain formation is clearly disfavored. Indeed, thiaoxadiphosphetane was formed during the AIMD simulation of this system. The energetics for the MeSP(S)O system also indicate that dimerization is clearly favored over chain formation, both kinetically and thermodynamically. This is consistent with the results of the AIMD simulations, where the formation of a thiaoxadiphosphetane was observed. Interestingly, the dimerization products of MeSP(S)O are unstable with respect to the reactant species at 500 K, and hence, it is unlikely that the dimers of this MTP molecule will exist at elevated temperatures.

a.iii. Analysis of the Electronic Structures of the MTPs. The AIMD simulations and static DFT calculations indicated that the $MeSPO_2$ system may take part in either of reactions **1** or **2** while the other three MTP molecules are only likely to dimerize. In this section, these differences are rationalized in terms of the electronic structures of these molecules.

The ESP-derived atomic charges[47−49] and HOMO and LUMO orbitals of the alkyl MTP molecules considered in

(47) Breneman, C. M.; Wiberg, K. B. *J. Comput. Chem.* **1990**, *11*, 361.
(48) Woods, R. J.; Khalil, M.; Pell, W.; Moffat, S. H.; Smith, V. H., Jr. *J. Comput. Chem.* **1990**, *11*, 297.
(49) Chirlian, L. E.; Francl, M. M. *J. Comput. Chem.* **1987**, *8*, 894.

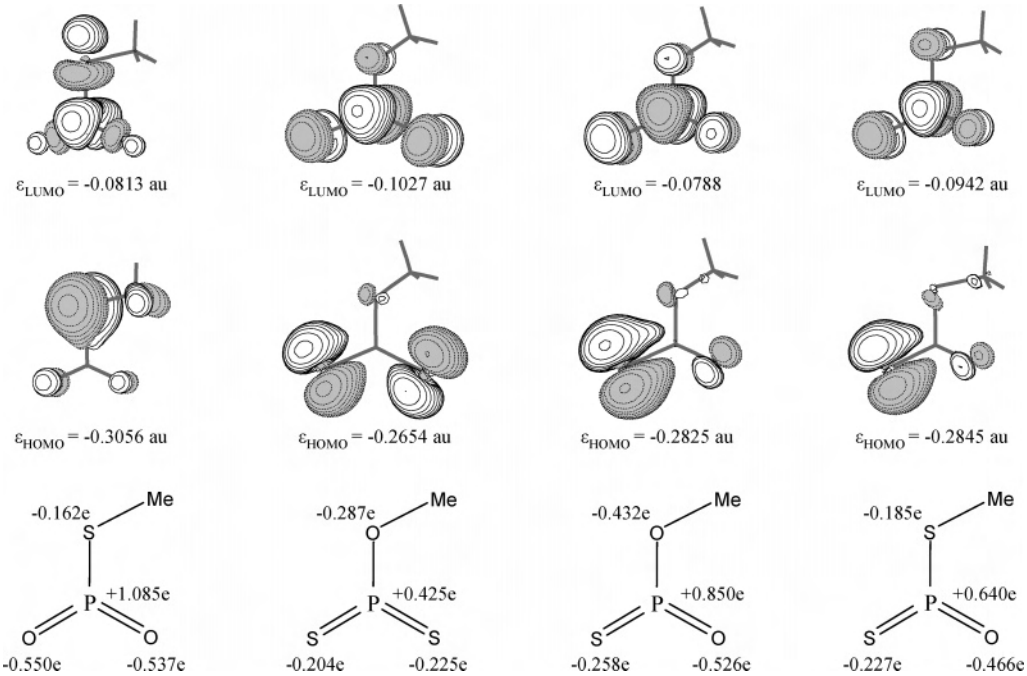

Figure 7. Relevant atomic charges and HOMO and LUMO orbitals for the alkyl MTPs considered in this study. Each column represents the data for one type of alkyl MTP, with the charges, HOMO orbital, and LUMO orbital given in the lower, middle, and upper structures, respectively. In all cases, the orientation of the molecules is consistent with that shown in the lower structure. All isosurfaces are plotted at a value of 0.05 au.

this study are shown in Figure 7. The charges affect the behavior of the molecules at large intermolecular distances, while the short-range behavior is dictated by orbital interactions. Before proceeding with the analysis of these data, it will be useful to consider which aspects of the electronic structures of these systems are necessary for the chain formation and dimerization reactions to occur. Reaction **1** occurs through the transfer of an alkoxy or sulfide group between the two phosphorus atoms, along with the formation of a P−O−P or P−S−P linkage. This reaction involves the dissociation of a P−O or P−S σ-bond and formation of another P−O or P−S σ-bond. Thus, in molecules that are likely to react according to reaction **1**, one would expect to find an electronic structure conducive to the formation and dissociation of P−S or P−O σ-bonds. Reaction **2**, on the other hand, primarily involves changes in the π-orbital structure of the system, and hence, the frontier orbitals of the MTP molecules that dimerize should exhibit π-character.

The HOMO of $MeSPO_2$ clearly corresponds to a lone-pair orbital on sulfur, while the LUMO consists of an antibonding σ-orbital between the P and S atoms, with small contributions from the oxygen atoms. The atomic charges indicate that P−O interactions will dominate in the early stages of the reaction between two of these molecules, which is consistent with the adduct observed during the AIMD simulation and located through the static DFT calculations. As the reaction proceeds, electron density will be transferred into the LUMO of one of the MTP molecules, which will prompt the dissociation of the P−S bond. As this occurs, the HOMO of one of the MTP molecules will interact with unoccupied orbitals on the phosphorus atom of the other to initiate the formation of a new P−S bond. Overall, this suggests that the electronic structure of $MeSPO_2$ favors sulfide transfer, which leads to chain formation through reaction **1**.

The frontier orbitals of $MeOPS_2$, MeOP(S)O, and MeSP(S)O are clearly different than those of $MeSPO_2$. The most relevant aspect of these data with respect to dimerization or chain formation is that the LUMO of each of these MTP molecules is of antibonding π-character. For the MeOP(S)O and MeSP(S)O molecules, the atomic charges favor initial interactions between the phosphorus and oxygen atoms. In the case of $MeOPS_2$, the P−O interaction is favored slightly by the atomic charges, which is consistent with structure observed during the early stages of the AIMD simulation of the system composed of two of these molecules. This would imply that alkoxy group transfer may occur; however, the orbital structure clearly disfavors this process. For each of these three types of MTPs, bond formation occurs through the donation of electron density into the LUMO, which in turn, leads to the dissociation of P−S or P−O π-bonds. As noted above, this favors dimerization, which is consistent with the results of the AIMD simulations and static DFT calculations.

b. Reactions between MTPs and Diphosphates. The AIMD simulations and static DFT calculations presented in the preceding section led to the identification of two reaction pathways for the formation of diphosphate structures from systems composed of two identical MTP molecules. In this section, the possible formation of longer phosphate chains through the reaction of these diphosphate products with additional MTP molecules is considered. The calculations performed to examine these processes will be of a more focused nature than in the previous section, with only representative examples of diphosphate chains and dimers being considered. Specifically, a system composed of an $MeSPO_2$ molecule reacting with $O_2P-O-P(O)(SMe)_2$ (the diphosphate chain formed from $MeSPO_2$ through reaction **1**) will be used to investigate the elongation of the products

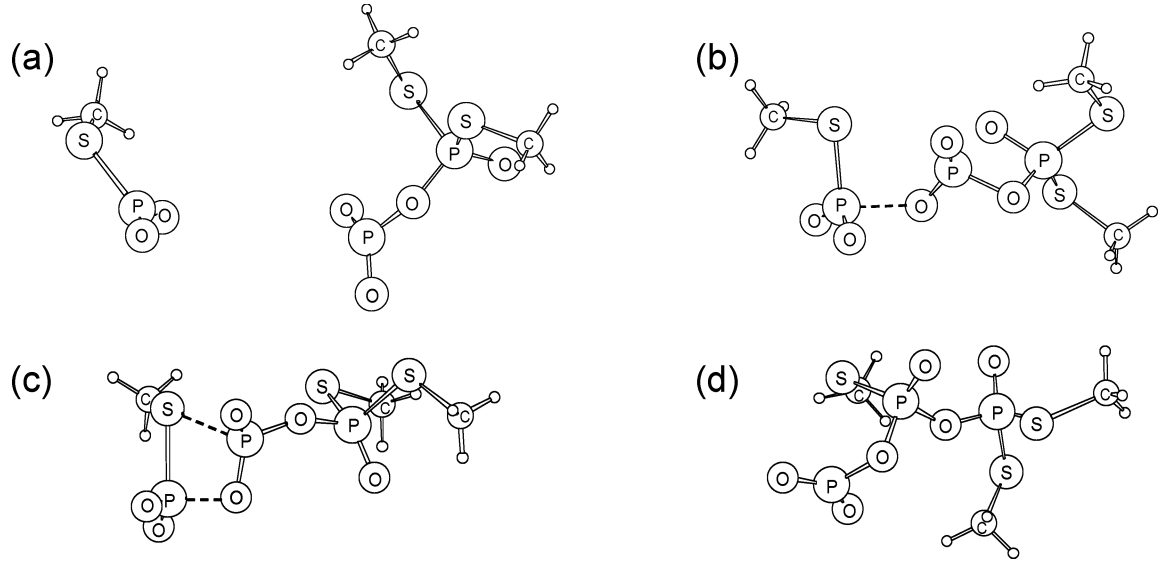

Figure 8. Key structures observed during the reaction of $MeOPS_2$ with the tri-coordinate phosphorus atom of $O_2P-O-P(O)(SMe)_2$. In (a) through (c), the distance between the phosphorus atom of $MeOPS_2$ and the tri-coordinate phosphorus atom of $O_2P-O-P(O)(SMe)_2$ is constrained. In (a), the two molecules are separated by a significant distance. The structure in (b) shows the initiation of P−O−P linkage formation between the two molecules. In (c), the system has attained a configuration allowing for simultaneous formation of the P−O−P linkage and transfer of the sulfide group. The final product, obtained after the removal of the geometric constraints, is shown in (d).

of chain formation and the addition of $MeOPS_2$ to $MeO(S)PS_2P(S)OMe$ (the dimer of $MeOPS_2$ formed through reaction **2**) will be considered to study the formation of larger phosphates from the dimers. These systems were selected on the basis of the results of the calculations presented in Section a, which showed that the $MeSPO_2$ system could undergo either of reactions **1** or **2**, while the other three MTP systems are only expected to dimerize.

AIMD simulations were performed to identify and examine the qualitative details of the reactions in which these systems take part to yield longer phosphate chains. The results of these simulations are presented in Section b.i. Overall, it was found that triphosphate chains can be formed through the addition of $MeSPO_2$ to either of the phosphorus atoms in $O_2P-O-P(O)(SMe)_2$ through processes similar to reaction **1**. On the other hand, it was found that the reaction of $MeOPS_2$ with $MeO(S)PS_2P(S)OMe$ does not lead to chain formation. Static DFT calculations were then performed to examine the observed reactions that led to the formation of longer phosphate chains in a more quantitative manner. The results of these calculations are presented in Section b.ii.

b.i. AIMD Simulations of Systems Composed of One Alkyl MTP and a Diphosphate. In Section a, it was noted that the diphosphate chain $O_2P-O-P(O)(SMe)_2$, formed when two $MeSPO_2$ molecules react according to reaction **1**, is of particular interest within the context of phosphate chain formation because it contains a tri-coordinate phosphorus atom that is a potential site for further chain formation reactions to take place. To examine this possibility, an AIMD simulation was performed on a system composed of one $MeSPO_2$ molecule and the $O_2P-O-P(O)(SMe)_2$ chain. Geometric constraints were employed such that the distance between the tri-coordinate phosphorus atom in the chain and the phosphorus atom in the MTP molecule decreased from an initial value of 7 Å only if the forces on the nuclei allowed this to occur naturally. The results showed that the length of the phosphate chain could increase through a reaction involving the transfer of a sulfide group and formation of a P−O−P linkage between the MTP and $O_2P-O-P(O)(SMe)_2$ molecules. This process is analogous to reaction **1**.

Structures along the calculated trajectory demonstrating the formation of the triphosphate product are shown in Figure 8. The structure in Figure 8a shows the initial configuration of the system, where the two molecules are separated by a large distance as a result of the geometric constraints. It was observed that these two molecules interacted initially through the phosphorus atom of $MeSPO_2$ and one of the oxygen atoms bonded to the tri-coordinate phosphorus atom in the diphosphate chain, as shown in Figure 8b. This interaction eventually led to the formation of a P−O−P linkage, which prompted the transfer of a sulfide group from the MTP molecule to the diphosphate chain through the structure shown in Figure 8c. The final product is shown in Figure 8d and was obtained by removing the geometric constraints after the reaction occurred and continuing the simulation for 2 ps. Overall, this reaction is analogous to the chain-formation process that was observed during the simulation of two $MeSPO_2$ molecules discussed in Section a. It is interesting to note that the tri-coordinate phosphorus atom is regenerated through this process, which indicates that elongation of the triphosphate product could take place through analogous reactions with additional $MeSPO_2$ molecules.

The $O_2P-O-P(O)(SMe)_2$ molecule also contains a tetra-coordinate phosphorus atom, which is a potential site for reactions with $MeSPO_2$ molecules to yield a triphosphate. To examine this possibility, a second AIMD simulation of the system composed of one $MeSPO_2$ molecule and one $O_2P-O-P(O)(SMe)_2$ molecule was performed, where the geometric constraints were applied to the distance between the phosphorus atom of the MTP molecule and the tetra-coordinate phosphorus atom of the diphosphate chains. The results of this simulation showed that the MTP molecule

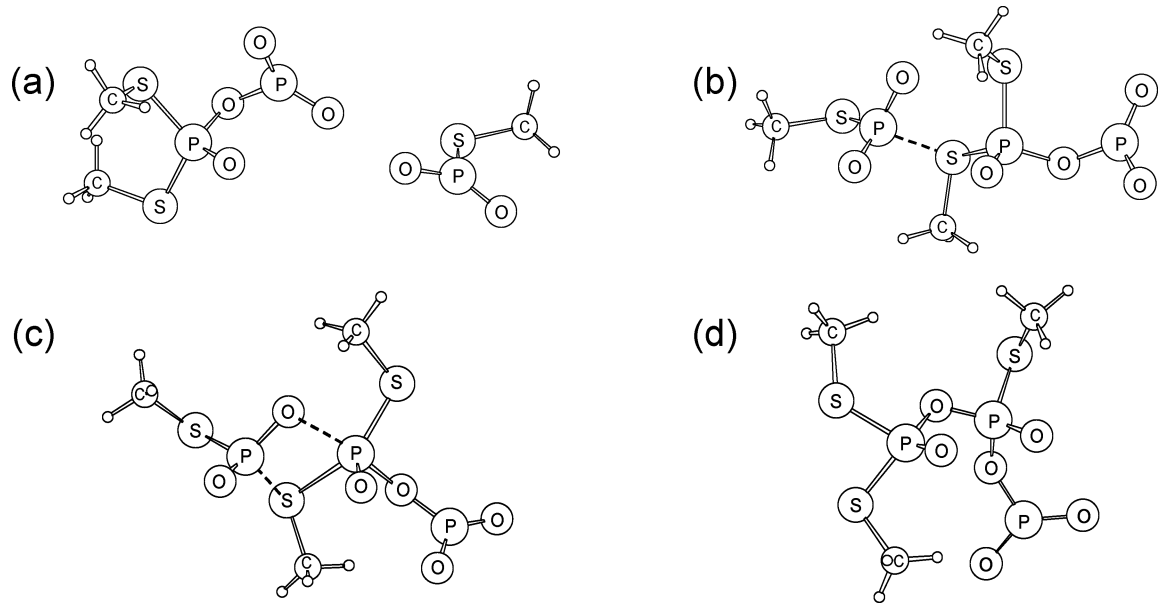

Figure 9. Key structures observed during the reaction of $MeOPS_2$ with the tetracoordinate phosphorus atom of $O_2P-O-P(O)(SMe)_2$. In (a) through (c), the distance between the phosphorus atom of $MeOPS_2$ and the tetracoordinate phosphorus atom of $O_2P-O-P(O)(SMe)_2$ is subject to geometric constraints. In (a), the two molecules are separated by a significant distance. The structure in (b) shows the initiation of P−S interaction between the two molecules. In (c), the system has attained a configuration allowing for simultaneous formation of the P−O−P linkage and transfer of the sulfide group. The final product, obtained after the removal of the geometric constraints, is shown in (d).

could react at the tetracoordinate phosphorus atom of $O_2P-O-P(O)(SMe)_2$ to form a triphosphate chain. Structures observed throughout the simulation that demonstrate this process are shown in Figure 9. The initial structure, in which the two molecules were well-separated, is shown in Figure 9a. As the intermolecular distance decreased, the molecules interacted through one of the sulfur atoms bonded to the tetracoordinate phosphorus atom in the chain and the phosphorus atom in the MTP molecule, as shown in Figure 9b. This contrasts with the reaction at the tri-coordinate phosphorus atom, where P−O interactions were dominant in the early stages of the reaction. The system eventually attained a configuration that allowed for the transfer of a sulfide group from the diphosphate chain to the MTP molecule, which occurred along with the formation of a P−O−P linkage, as shown in Figure 9c. The final product of this reaction, shown in Figure 9d, was obtained by continuing the simulation without geometric constraints for 2 ps after the reaction took place and is identical to that shown in Figure 9d. It is interesting to note that the product of this reaction also contains a tetracoordinate phosphorus atom that is a potential site for analogous reactions with additional MTP molecules to take place to form longer phosphate chains.

It is also of interest to consider the reactions that can occur between the MTP molecules and the diphosphate dimers. As noted above, a system composed of one $MeOPS_2$ molecule and the $MeOPS_2$ dimer will be considered as a representative system upon which to perform simulations to gain insight into such reactions. The two phosphorus atoms in the dimer are equivalent, and hence, only one AIMD simulation was performed for this system, where the distance between the phosphorus atom in the MTP molecule and one of the phosphorus atoms of the dimer was constrained as described above. The results showed that the introduction of the MTP molecule resulted in the decomposition of the dimer through the elimination of an MTP molecule, which was followed by the formation of a new dimer. Overall, this reaction does not lead to the formation of a triphosphate chain, but rather regenerates the reactant species, i.e., one $MeOPS_2$ molecule and one $MeO(S)PS_2P(S)OMe$ dimer. It is assumed that the other MTP dimers will react in a similar manner.

b.ii. Static DFT Calculations of the Reactions between $O_2P-O-P(O)(SMe)_2$ and $MeSPO_2$. The AIMD simulations of the system composed of one $MeSPO_2$ molecule and one $O_2P-O-P(O)(SMe)_2$ diphosphate chain showed that these two species can react to yield a triphosphate chain through either of two reactions. These processes are similar to reaction **1** in that they both involve P−O−P linkage formation along with the transfer of a sulfide group between phosphorus atoms. In the first case, the addition of $MeSPO_2$ occurs at the tri-coordinate phosphorus of the growing phosphate chain, while the other involves addition at the tetracoordinate phosphorus atom. In this section, the structural and energetic details of the key structures along these reaction pathways will be evaluated through static DFT calculations at the B3LYP/6-311+G(d,p) level of theory. The reactions considered will be limited to those that occur between an $MeSPO_2$ molecule and the $O_2P-O-P(O)(SMe)_2$ chain because the results presented in Section a suggested that $MeSPO_2$ is the only MTP molecule considered in this study that is likely to take part in chain formation. The structures of the stationary points located along these two reaction pathways are shown in Figure 10, and the energetics associated with these structures are given in Table 3.

The structural data given in Figure 10 show that the addition of $MeSPO_2$ to $O_2P-O-P(O)(SMe)_2$ at the tri-coordinate phosphorus atom involves the initial formation

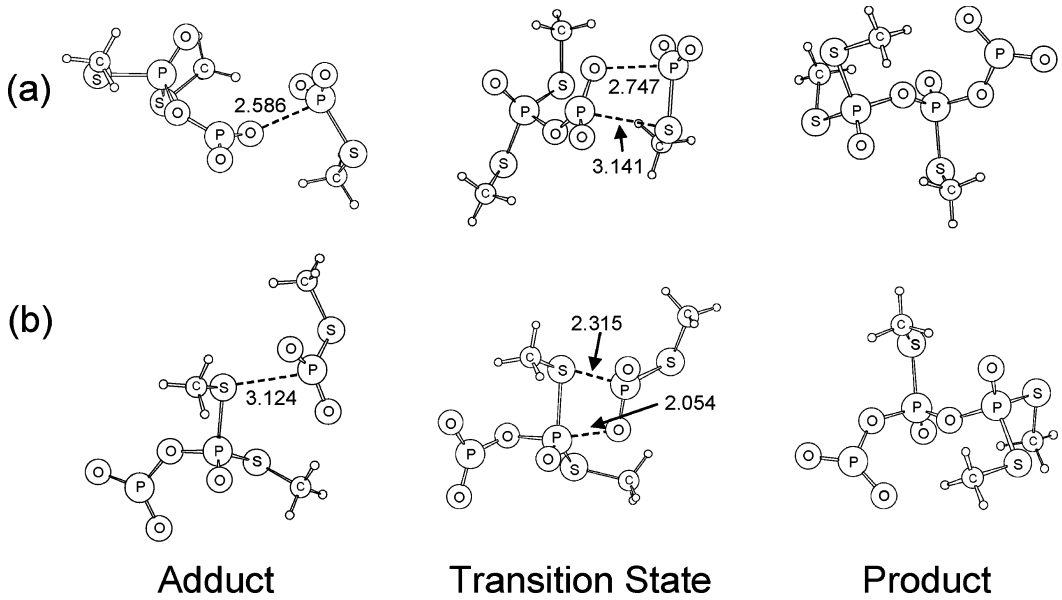

Figure 10. Structures of the stationary points along the reaction pathways for the reaction of the $O_2P-O-PO(SMe)_2$ polymer with $MeSPO_2$. In (a), the structures along the reaction pathway are shown for the addition of $MeSPO_2$ at the tri-coordinate phosphorus atom of the diphosphate chain. In (b), the corresponding structures are shown for the reaction at the tetracoordinate phosphorus atom of the diphosphate chain. All distances are in Å.

Table 3. Relative Electronic and Free Energies[a,b] for the Addition of $MeSPO_2$ to the Tri- and Tetracoordinate Phosphorus Atoms of $O_2P-O-P(O)(SMe)_2$

species	ΔE	ΔG^{500K}	ΔG^{1000K}
Reaction at Tri-coordinate P			
adduct	−6.1	18.9	48.3
transition state	−3.3	22.8	50.7
product	−25.4	0.8	27.3
Reaction at Tetracoordinate P			
adduct	−4.4	21.8	50.0
transition state	10.8	38.8	69.1
product	−25.4	0.8	27.3

[a] All energies are in kcal/mol relative to separate reactant molecules at the B3LYP/6-311+G(d,p) level of theory and include ZPVE corrections. [b] The superscripted numbers on the free energy headings indicate the temperature at which the free energy was calculated.

of an adduct, where the primary intermolecular interaction is between the phosphorus atom of the MTP molecule and an oxygen atom bonded to the tri-coordinate phosphorus atom of the diphosphate chain. In the transition state, this P−O distance has increased slightly, while the distance between the tri-coordinate phosphorus atom of the diphosphate chain and the sulfur atom in $MeSPO_2$ has decreased significantly. The transition-state structure is consistent with the simultaneous formation of the P−O−P linkage and transfer of the sulfide group between the two molecules. The product of this reaction is a triphosphate chain that contains a tri-coordinate phosphorus atom where reactions with additional MTP molecules could potentially take place to form longer phosphate chains.

The addition of the MTP molecule to the tetracoordinate phosphorus atom of $O_2P-O-P(O)(SMe)_2$ involves the initial formation of an adduct structure where one of the sulfur atoms that are bonded to the tetracoordinate phosphorus atom of the diphosphate chain interacts with the phosphorus atom of the incoming MTP molecule. In the transition state, this P−S distance has decreased significantly and the formation of a P−O−P linkage has been initiated. Overall, the transition state is consistent with a process involving the simultaneous transfer of a sulfide group and the formation of a P−O−P linkage between the two molecules. The product of this reaction is identical to that formed through the addition of $MeSPO_2$ to the tri-coordinate phosphorus atom of $O_2P-O-P(O)(SMe)_2$ and contains a terminal tetracoordinate phosphorus atom that is a potential site for elongation of the triphosphate chain through analogous reactions with additional MTP molecules.

The electronic potential energies and free energies of the stationary points along the two chain formation reaction pathways are given in Table 3 relative to the energies of the separated $MeSPO_2$ and $O_2P-O-PO(SMe)_2$ molecules. Since the products of these two reactions are identical, the thermodynamic data are not particularly useful in determining which reaction pathway is favored. The calculated barrier for the addition at the tri-coordinate phosphorus atom is significantly lower than that for addition at the tetracoordinate phosphorus atom, which indicates that the former is favored kinetically. This is not surprising considering that, among other factors, the incoming MTP molecule will encounter minimal steric repulsion at the tri-coordinate phosphorus atom, while the approach of the MTP molecule at the tetracoordinate phosphorus atom will be sterically hindered. Thus, the growth of the phosphate chains is likely to occur through the addition of $MeSPO_2$ molecules at the tri-coordinate phosphorus atom of the diphosphate polymer. This reaction forms the basis of the phosphate polymerization schemes that will be developed in the next section.

c. Mechanism for the Formation of Phosphates from ZDDP. The results presented in Section a showed that bimolecular systems of MTP molecules can either form phosphate chains (reaction **1**) or dimerize (reaction **2**). In Section b, the reactions that occur between MTP molecules and the products of reactions **1** and **2** were also explored. In that section, it was found that the diphosphate chains formed

Scheme 2. Reaction Mechanism Linking ZDDP Additives to Linear Phosphate Chains[a]

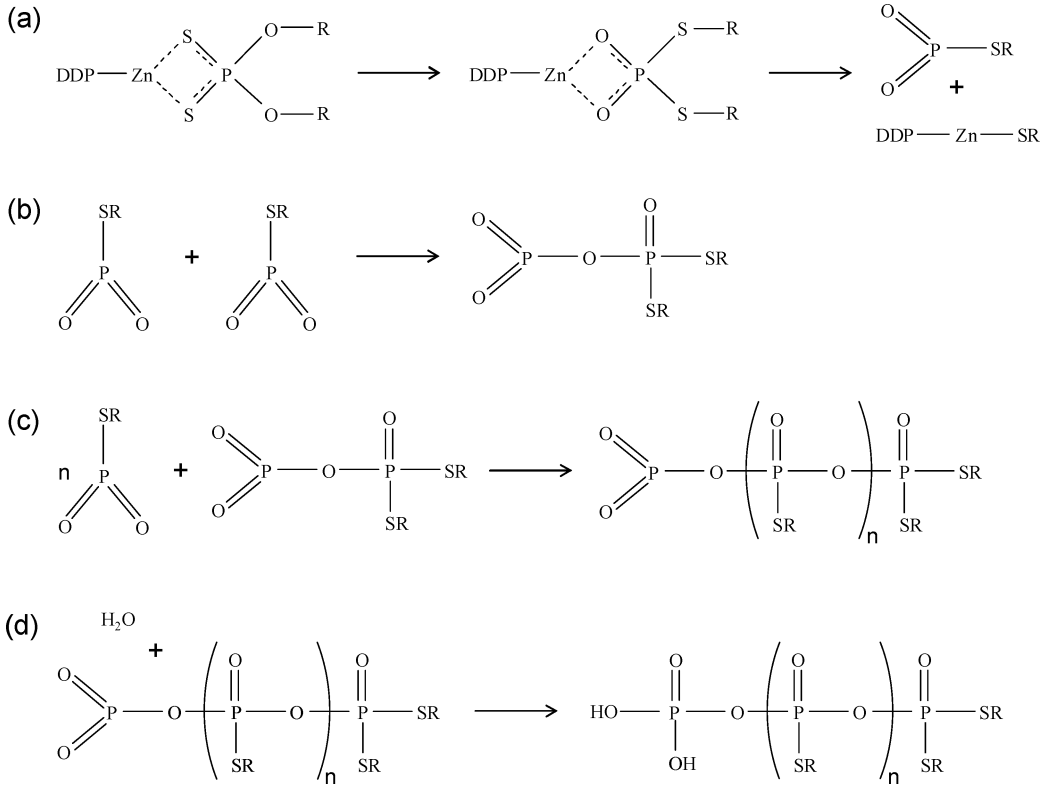

[a] The details of steps (a) through (d) are described in the main text. R = an alkyl group and DDP = $S_2P(OR)_2^-$.

through reaction **1** could react with additional MTP molecules to yield longer phosphate chains through a process that is analogous to reaction **1** and regenerates the tri-coordinate phosphorus atom. On the other hand, the results presented in Section b indicated that the dimers did not take part in reactions that yielded longer phosphate chains. The possibility of forming phosphate chains through successive occurrences of reaction **1** is intriguing within the context of transforming ZDDP antiwear additives into ZDDP antiwear films, which are composed of zinc phosphates. This is particularly true because the reagents for reaction **1**, i.e., MTP molecules, are derived from ZDDP. In this section, reactions **1** and **2** will be used to establish a general reaction scheme that connects the ZDDP molecule to linear phosphate chains. The details of this reaction mechanism are outlined in Scheme 2. In the remainder of this section, the qualitative aspects of this reaction mechanism will be described first and the energetic details associated with these reactions will follow. It is noted that, while we present this mechanism within the context of our own interest in ZDDP antiwear additives, it may be of more general use in the formation of other complex phosphate structures.

The proposed reaction mechanism linking ZDDP additives to linear phosphate chains is shown in Scheme 2. In step (a), the ZDDP molecule first isomerizes to yield LI2 and then decomposes through the elimination of $RSPO_2$. These processes have been discussed in detail in studies reported previously.[17,20,21] In step (b), the $RSPO_2$ molecules take part in reaction **1** to yield a diphosphate chain that contains a tri-coordinate phosphorus atom. The extent to which this reaction will occur is dependent upon the relative energetics of reactions **1** and **2**, which are discussed later in this section. In step (c), additional MTP molecules present in the oil react with the tri-coordinate phosphorus atom of the growing phosphate chain through the analogue of reaction **1** that was discussed in Section b. Step (c) forms the basis of the polymerization mechanism. As indicated in Scheme 2, for every n MTP molecules added to the diphosphate chain formed in step (b), a phosphate chain of length $n + 2$ is generated. The addition of multiple MTP molecules to the diphosphate chain is proposed to occur through a process in which one MTP molecule reacts with the tri-coordinate phosphorus atom of the diphosphate chain to yield a triphosphate chain, which also contains a tri-coordinate phosphorus atom. Another MTP molecule can then react at the tri-coordinate phosphorus atom of the triphosphate chain to yield at tetraphosphate chain, while regenerating the tri-coordinate phosphorus center, and so on. The tri-coordinate phosphorus atom that is the reactive site for this polymerization scheme is a highly reactive, electrophilic center. As such, it is likely that the phosphate chains formed throughout steps (b) and (c) are unstable species that will react with other nucleophiles in the oil. Such reactions will saturate the coordination at the tri-coordinate phosphorus, i.e., this atom will become tetracoordinate, thereby terminating polymerization. This process is indicated in step (d) of Scheme 2, where the addition of water to the tri-coordinate phosphorus atom has been considered explicitly. This reaction seems particularly reasonable under engine conditions where water is formed in large quantities as a byproduct of combustion.

Overall, the steps shown in Scheme 2 form a reaction mechanism demonstrating how ZDDP decomposes into basic

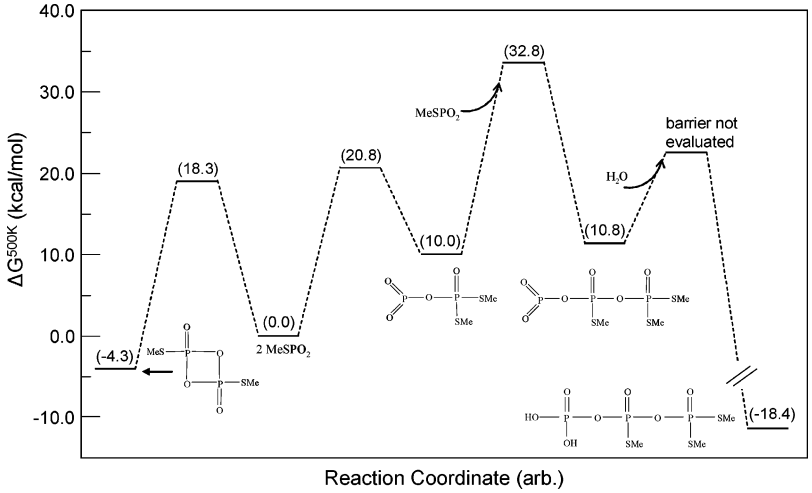

Figure 11. Relevant species and associated energetics for the formation of phosphate polymers from $MeSPO_2$ molecules. The energies of the intermediates, transition states and products are indicated in kcal/mol in brackets.

phosphate building blocks that are subsequently transformed into phosphate chains. These processes are akin to free-radical polymerization, where stable molecules decompose to form highly reactive radicals, which then react with monomers to yield unstable intermediate polymers of longer chain lengths through processes that regenerate the reactive center until some termination reaction occurs. Here, the stable molecules are ZDDPs, which decompose into reactive MTP species. The MTPs then take part in a polymerization process that forms phosphate chains until the site at which polymerization occurs, i.e., the tri-coordinate phosphorus atom, is saturated through attack by a nucleophile in the oil. In what follows, the energetic details associated with these processes will be explored.

The extent to which the polymerization mechanism shown in Scheme 2 will occur is dependent upon the energetics associated with the reactions in which $MeSPO_2$ molecules can take part. $MeSPO_2$ molecules are formed through the decomposition of ZDDP isomers at locations where engine surfaces come into contact and temperatures approach 1000 K. As argued in Section a.ii., these molecules should not react with other species until they encounter regions where the temperature is ~500 K or lower, which should allow appreciable quantities of MTP molecules to accumulate in engine oil. As such, the following analysis will focus on processes occurring within systems composed exclusively of MTP molecules. The reader is directed to our earlier studies[17,20,21] for a discussion of the energetics associated with the formation of MTPs, which must precede the processes discussed in what follows.

The free energies at 500 K are given in Figure 11 for reactions leading to the formation of a triphosphate from three $MeSPO_2$ molecules and water according to the polymerization mechanism outlined in Scheme 2. When two $MeSPO_2$ molecules encounter one another, they can react according to either of reactions **1** (chain formation) or **2** (dimerization). The energetics show that dimerization is preferred at this temperature, with the dimer being favored over separated monomers by 4.3 kcal/mol. However, in Section b, it was demonstrated that reactions between the dimer and an MTP monomer simply yields another dimer and monomer. Consequently, dimers will persist in the oil and eventually establish an equilibrium with the separate monomers. The calculated energetics suggest that when such an equilibrium is reached, ~1% of the MTP molecules will be present in the monomeric form. The monomers can react to yield a diphosphate chain through reaction **1**, which will remove monomers from the system and prompt further decomposition of the dimers. As such, the dimers can be thought of as a source of MTP molecules and the chain formation reactions as a sink for these molecules. The energetics clearly demonstrate that the diphosphate chain is less stable than the monomers. This chain can either decompose to re-form the separate monomers or react with additional MTP molecules to yield an even longer phosphate chain. Decomposition will essentially allow the entire process to start over again. On the other hand, elongation of the chain destabilizes the system by another 0.8 kcal/mol, indicating that, although the continual addition of MTP molecules to the growing chain is possible, this process does not yield stable phosphate chains. This is consistent with the analogy to free-radical polymerization mentioned above, where the intermediate species formed throughout the polymerization process are inherently unstable. The formation of a stable phosphate polymer can be achieved through attack of the tri-coordinate phosphorus atom in the growing chain by a nucleophile in the oil. As noted above, this will increase the coordination number at the reactive phosphorus atom to four, thereby stabilizing the system and preventing further chain growth. In Figure 11, the addition of water is considered as a termination reaction and was found to stabilize the system by 29.2 kcal/mol, which is sufficient to render the final triphosphate product energetically favorable with respect to the reactant molecules. The energetic barrier for the addition of water was not evaluated; however, it is reasonable to assume that it is similar to, or smaller than, those for the other reactions considered here and hence is accessible under engine conditions. Overall, these reactions provide a plausible means of transforming ZDDP additives into phosphate chains.

Using the energetics for these reactions, it is possible to estimate an upper limit on the lengths of the phosphate chains formed through this polymerization mechanism. Assuming that the addition of water to the growing phosphate chain stabilizes the system by approximately 30 kcal/mol and the addition of each MTP molecule to the growing phosphate chain destabilizes the system by 0.8 kcal/mol (the difference in energies of the di- and triphosphate chains), it is possible to place an upper limit of approximately 24 units on the length of the phosphate polymers formed through this mechanism. The consideration of other termination reactions may change this value. In light of the energetics in Figure 11, which indicate that the system becomes increasingly unstable with the chain length, it seems appropriate to suggest that this reaction mechanism can lead to phosphate chains that contain between 2 and 24 phosphate units with a preference for shorter chains. In a broad sense, these chain lengths are consistent with those reported previously for ZDDP antiwear and thermal films, which range from ~3 to 20 phosphate units in length.[50,51]

Thus, the reactions described in Sections a and b, along with the decomposition and isomerization of ZDDP as described previously, form a reaction scheme that connects the ZDDP molecule to linear phosphate chains, which may be precursors to the antiwear films. It is noted that the entire polymerization scheme described above is based on the notion that the $MeSPO_2$ dimer persists in the oil as a stable species and acts as a source of $MeSPO_2$ monomers. This was justified on the basis that reacting the dimer with additional MTP molecules does not yield larger phosphate species, e.g., a trimer or triphosphate chain. It should be mentioned, however, that the dimer does indeed react with the other MTP molecules, yet only forms a new dimer and liberates an MTP monomer. That is, the reactants and products in such a process are identical to one another and contain an MTP monomer. If the MTP dimer should react with a different species, e.g., water, two products would be formed. In the specific case of the reaction between the $MeSPO_2$ dimer and water, the first product would be a phosphate, $PO(OH)_2(SMe)$, and the second would be an $MeSPO_2$ monomer. Thus, the reaction of the MTP dimers with other species in the oil also liberates MTP monomers, which will enable the polymerization scheme described above.

IV. Conclusions

The reactions that can occur within systems composed of MTP molecules have been explored through AIMD simulations and static DFT calculations. The results of these calculations led to the identification of two reactions in which these systems can take part to yield more complex phosphate structures. The first of these reactions simply involves the dimerization of two MTP molecules and has been reported in previous experimental studies. The second reaction involves the transfer of a sulfide group and formation of a P−O−P linkage between the tri-coordinate phosphorus atoms of the MTP molecules to yield a longer phosphate chain. This process regenerates the reactive center within the molecule and, to the best of our knowledge, has not been reported previously.

It was found that the $MeSPO_2$ molecule could participate in either the dimerization or chain-formation reactions, with the former being preferred on longer time scales. On the other hand, the remaining three MTPs considered in this study are only likely to take part in dimerization. These differences can be understood in terms of the electronic structures of these systems. Simulations performed to explore the possible elongation of the phosphate products of these reactions showed that the dimers did not react with additional MTP molecules, while the length of the phosphate chains could be increased through reactions with additional MTP molecules. Overall, the results suggest that only $MeSPO_2$ should form such phosphate chains. This is interesting within the context of forming ZDDP antiwear films because it has been shown previously that $MeSPO_2$ is the MTP molecule that is most likely to be formed from ZDDP.

The details of the dimerization and polymerization reactions were used to develop a reaction scheme linking MTP molecules to phosphate chains. Within this polymerization mechanism, it is likely that phosphate chains between 2 and 24 phosphate units in length will be formed, assuming that the reaction with water terminates polymerization. While it is not possible to conclude that the polymerization scheme developed in this study is a primary mode of phosphate formation within engines, the results point toward a pathway for the transformation of ZDDP antiwear additives into phosphates. This represents a significant step toward understanding how ZDDPs are transformed into phosphates, which may prove useful in the design of new antiwear additives. In a more general sense, this mechanism may be relevant to other systems that contain MTPs. In such cases, it may be possible to control the lengths of the phosphate chains formed through polymerization by, for instance, selecting a particular nucleophile other than water to terminate chain growth.

Acknowledgment. We gratefully acknowledge the Natural Sciences and Engineering Research Council of Canada (NSERC), General Motors Canada, and General Motors Research and Development for financial support. Computing resources were made available by the Canadian Foundation for Innovation, the Ontario Innovation Trust, SHARCNet of Canada, and the Academic Development Fund at the University of Western Ontario.

Supporting Information Available: Cartesian coordinates and energies. This material is available free of charge via the Internet at http://pubs.acs.org.

IC0608391

(50) Martin, J. M.; Grossiord, C.; Le Mogne, T.; Bec, S.; Tonck, A. *Tribol. Int.* **2001**, *34*, 523.
(51) Yin, Z. *Chemistry of Antiwear Films by X-ray Absorption Spectroscopy*; University of Western Ontario: London, Ontario, 1995.